

ADVANCED PRESSURE BOUNDARY MATERIALS

Michael Santella

Oak Ridge National Laboratory, 1 Bethel Valley Road, Oak Ridge, Tennessee, 37831-6096

Email: santellaml@ornl.gov; Telephone: 865-574-4805

John Shingledecker

EPRI, 1300 W. T. Harris Blvd., Charlotte, NC 28262

Email: jshingledecker@epri.com; Telephone: 704-595-2120

ABSTRACT

Creep-Strength-Enhanced Ferritic Steels (CSEF) commonly referred to P91, P911, P92, and P122 require fully martensitic microstructures for optimum properties, mainly good creep strength. However, broad chemical compositional ranges are specified for these steel grades which can strongly influence the microstructures obtained. In this study, we have produced chemical compositions within the specification ranges for these alloys, which intentionally cause the formation of ferrite or substantially alter the lower intercritical temperatures (A_i) so as to affect the phase transformation behavior during tempering. Thermodynamic modeling, thermo-mechanical simulation, tensile testing, creep testing, and microstructural analysis were used to evaluate these materials. The results show the usefulness of thermodynamic calculations for setting rational chemical composition ranges for CSEF steels to control the critical temperatures, set heat-treatment temperature limits, and eliminate the formation of ferrite.

INTRODUCTION

Creep-strength-enhanced ferritic (CSEF) steels commonly referred to as P91, P911, P92, and P122 are being widely utilized for power-generation applications including fossil-fired boilers, heat-recovery steam generators, and petrochemical plants because they offer increased creep strength and oxidation resistance compared to standard Cr-Mo steels such as ASTM A387 Grades 11 and 22. However, numerous failures of CSEF steels have been reported after very short-time operation where the causes of failure have been identified at every level of the supply chain including at the material suppliers [1], in the fabrication shops [2,3], and during field erection [4,5]. Other studies have identified shortened creep life, below the expected design life, in properly processed CSEF steels due to unfavorable chemical compositions within the alloy specification ranges [6,7]. Thus, there is a desire to better understand how the specified chemical composition ranges for these alloys can affect transformation behavior and produce unfavorable microstructures which lead to reduced mechanical properties and ultimately premature failure of components.

CSEF steels require a 100% tempered martensitic structure for optimum creep properties. Kimura et al. have shown the presence of ferrite in these steels can dramatically reduce creep strength due to a large C and N concentration gradients between the tempered martensite grain and the ferrite. These compositional gradients accelerated the formation of coarse precipitates in this region, promoting recovery of the structure which led to local weakening [8]. Masuyama et al. observed that heat-treating these steels near or even below the experimentally determined lower critical temperature, A_{c1} , will have a negative effect on the creep resistance of the alloy [9]. Ryu et al found that improper heat-treatments can cause substantial changes in hardness and microstructure, which resulted, for some cases, in dramatic reductions in creep strength [10].

In this study, we present the results of our initial exploration to evaluate the extremes of the specified compositional ranges for P91, P92, and P122 using computational thermodynamics (CT) to

intentionally produce materials which form ferrite or extremely low intercritical temperatures (A_1). Our experimental results indicate that CT accurately predicts the phase transformation behavior and microstructures we observe and thus constitutes a powerful tool for specifying more stringent compositional ranges for these alloys. Preliminary suggestions for the specification range of Grade 91 are also presented.

EXPERIMENTAL DETAILS

Two compositions of each P91, P92, and P122 were produced via arc-melting in 25 x 25 x 125mm copper molds. Chemical analysis was performed after homogenization at 1200°C for 8 hours in vacuum. The castings were processed by successive hot rolling steps (10% reductions) at 700°C to 6.4mm thick plate. The plates were austenitized at 1050°C for 1 hour followed by air cooling and then tempered at 760°C for 1 hour. The aim chemistries for each alloy were based on the compositional limits of ASTM A387 Grade 91 for P91, ASME Code Case 2179 for P92, and ASME Code Case 2180 for P122. The intention was to produce one heat of each alloy with the austenite-forming elements (C, Mn, Ni, Cu, N) at the maximum of the range and the ferrite-forming elements (Si, Cr, Mo, W, V, Nb) at the minimum of the range and a second heat of each with the variations reversed. Phase stability as a function of temperature was calculated using Thermocalc™ with a standard Fe-database [11]. Solid round bars, 6.3mm dia., were machined from each alloy for thermo-mechanical evaluation in a Gleeble™ testing machine. Simulations were performed at a heating rate of 1.67 °C/sec followed by a second run at 0.032 °C/sec (100°C/min and 2°C/min, respectively). Subsize round shoulder-loaded tensile-creep specimens were machined with a 3.2mm diameter and 28.6 mm gauge length. Tensile tests were performed at room temperature and 650°C; no extensometer was used at 650°C. Creep-rupture tests were conducted at 650°C and 100 to 150 MPa. Optical microscopy was performed to determine if ferrite was present in the microstructure.

RESULTS

TABLE 1. Composition of heats in this study

Heat Number	Alloy	C	Mn	Si	Cr	Mo	W	Ni	Cu	V	Nb	N
19836	91	0.110	0.62	<i>0.16</i>	8.12	0.81	0.08	<i>0.44</i>	0.02	0.167	<i>0.05</i>	<i>0.024</i>
19837	91	<i>0.041</i>	0.25	0.53	9.63	<i>1.12</i>	0.01	0.01	0.01	<i>0.283</i>	0.11	<i>0.014</i>
19838	92	0.089	0.58	0.01	8.22	0.30	1.83	0.40	0.02	0.149	0.04	<i>0.020</i>
19839	92	<i>0.050</i>	0.34	0.46	9.42	0.58	<i>4.02</i>	0.01	0.02	0.240	0.08	<i>0.014</i>
19840	122	0.088	0.7	0.01	9.94	0.25	1.65	0.51	1.58	0.154	0.04	0.031
19841	122	<i>0.044</i>	0.03	0.48	<i>12.3</i>	0.59	<i>2.71</i>	0.01	0.29	0.284	0.10	<i>0.022</i>

The heat chemistries are listed in Table 1. Overall, the chemical compositions accurately reflected the minimum and maximum compositions in the alloy specifications. In a few cases, the range was exceeded (italicized in Table 1) but this did not typically exceed 10% of the maximum value. The only element poorly controlled by the vacuum arc-melting process was N, which was lower than the specified range for five of the six heats. For brevity, only the optical micrographs are shown for P91 in Figure 1, but the microstructures of P92 and P122 showed similar trends. Two different microstructures were observed for P91. For Heat 19836, designed to have a low intercritical temperature, the microstructure is 100% tempered martensite. For Heat 19837 designed to form ferrite, the microstructure shows a bimodal distribution of prior austenite grain boundaries containing a martensitic lath substructure and large ferrite grains that appear free of precipitation or

substructure. Figure 2 shows the Gleeble simulations performed on P91 Heat 19836 delineating the heating and cooling portions of each simulation and the location of the lower intercritical temperature, A_{c1} , and the martensite start temperature, M_s . As expected, the heating rate dependency of A_{c1} was observed where the A_{c1} is higher for the faster heating rate.

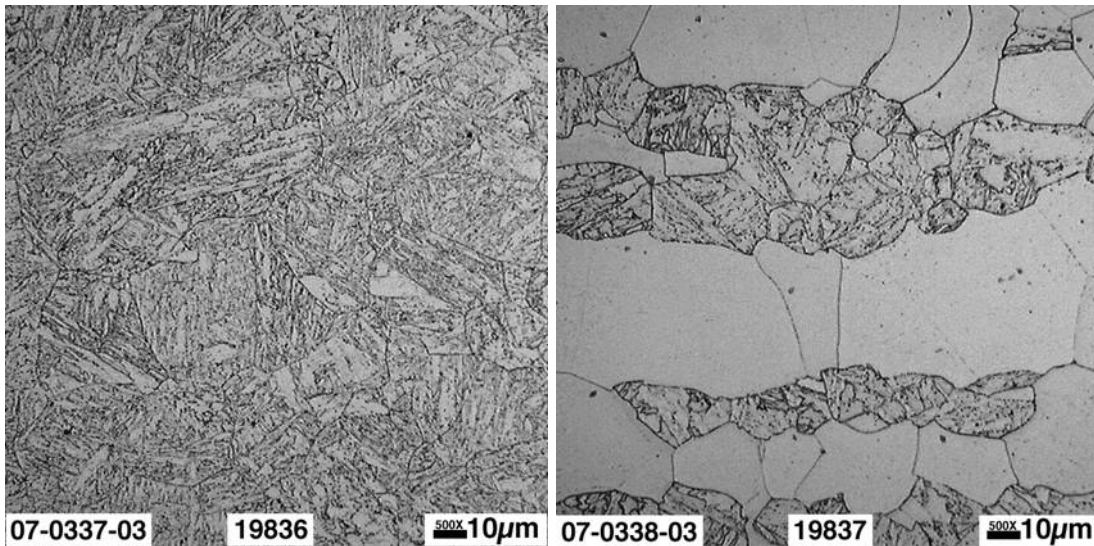


Figure 1. Optical micrographs of P91 Heat 19836 (left) with a typical 100% martensitic structure and Heat 19837 (right) containing ferrite

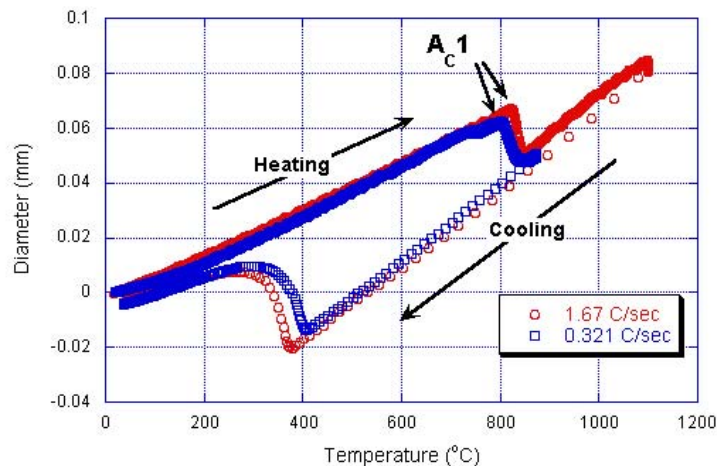


Figure 2. Temperature vs. diameter for P91 Heat 19836 showing the location for the experimentally determined A_{c1} temperature for two heating rates

A summary of all the optical microscopy performed on the normalized-and-tempered materials and the Gleeble simulations conducted on the 100% martensitic heats is given in Table 2. Included in Table 2 are the predicted behaviors of the alloys as determined by CT. For ferrite determination, the prediction of ferrite formation at the austenitization temperature (1050°C) matched the observed microstructures. For the intercritical temperatures, the predicted A_1 temperature was lower in all cases compared the measured A_{c1} temperatures. For P91 and P92, the difference was $\sim 20^{\circ}\text{C}$ but for P122 this difference was greater, $\sim 40^{\circ}\text{C}$.

The results of the room temperature and high-temperature tensile tests are shown in Figure 3. At room temperature, the heats containing ferrite displayed nearly identical stress-strain behavior with

very low tensile strength and good ductility (20-25%) regardless of alloy type. For the low intercritical alloys, P91 and P92 showed typical behavior with tensile strength of ~100 ksi (650 MPa) and ductilities in excess of 15%. However, the P122 showed very high tensile strength, nearly 130 ksi (840 MPa), with ductility below 15%. A similar trend was observed at 650°C where the alloys containing ferrite all had very low tensile strength. The tensile strength was separated in the same fashion for these alloys with the strength decreasing from P92 to P91 to P122. For the low intercritical alloys, again the P91 and P92 were similar and the P122 had very high tensile strength, in excess of 50 ksi (320 MPa), with the lowest ductility of all the materials.

TABLE 2. Comparison of experimental observations and thermodynamic predictions

Heat (alloy)	Ferrite Present?		Lower Critical Temperature		
	Experimental	Calculated	Experimental		Calculated
	Optical Microscopy	Ferrite at 1050°C	A _{c1} 100°C/min (°C)	A _{c1} (°C) 2°C/min	A ₁ (°C)
19836 (91)	No	No	811	790	775
19837 (91)	Yes	Yes	-	-	-
19838 (92)	No	No	804		783
19839 (92)	Yes	Yes	-	-	-
19840 (122)	No	No	792	771	739
19841 (122)	Yes	Yes	-	-	-

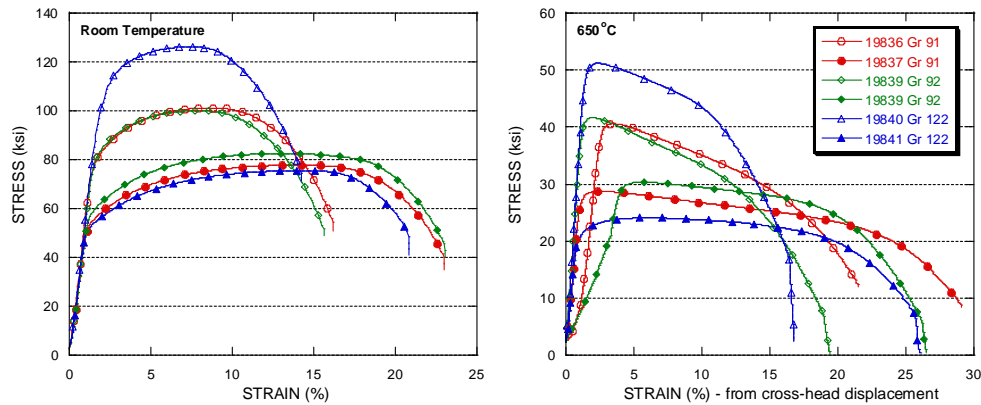


Figure 3. Tensile curves for all alloys at room temperature (left) and 650°C (right)

Figure 4 shows the time to rupture for all the creep-rupture tests conducted at 650°C. Four tests were conducted on both P91 compositions and three tests were conducted on each of the P92 and 122 compositions. A mean and minimum time to rupture line for P91 is included on the plot for comparison. In all cases, the alloys containing ferrite had inferior strength compared to the same alloy with the 100% tempered martensitic structure. For P91, the low intercritical temperature alloy met the average properties expected for P91, but three of the four tests conducted on the P91 with ferrite ruptured at times below the P91 minimum. For P92 at short-times, both alloys had similar rupture lives but at lower stress and longer test duration, the low intercritical alloy showed longer rupture time. Interestingly, the P92 containing ferrite showed similar strength to the P91 average properties. For the P122, a very wide variation in rupture time was observed. The P122 with ferrite had the lowest rupture life of any material tested, but the P122 with the tempered martensitic structure had the longest rupture life of any material with two tests continuing beyond 3,000 hours.

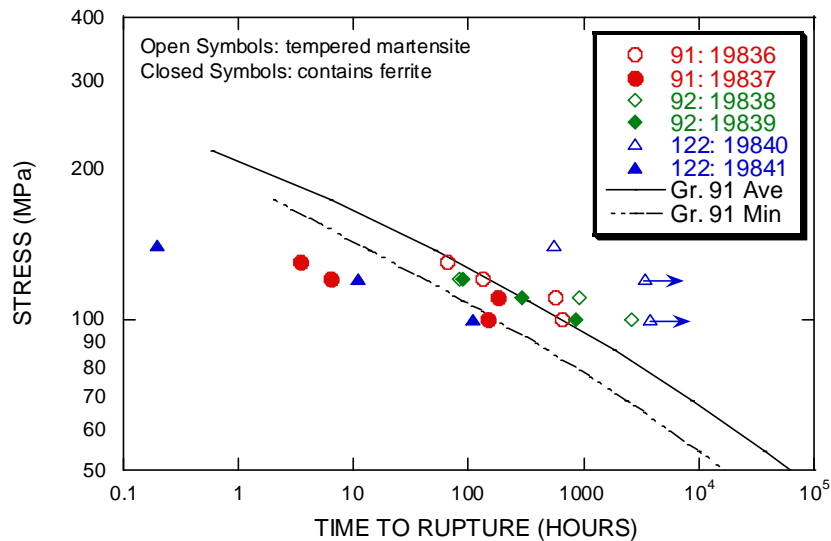


Figure 4. Creep-rupture life of alloys at 650°C (arrows indicate tests in progress)

DISCUSSION

An evaluation of the data in Table 2 shows that qualitatively the CT calculations are in good agreement with the experimental evidence for the formation of ferrite. A quantitative measurement for amount of ferrite, determined from optical microscopy, is given in Table 3. The amount of ferrite cannot be directly determined from the CT calculations because the amount of ferrite present at the M_s temperature will be greater than the amount at the austenitization temperature. This can be rationalized through evaluation of the phase stability calculations, shown for Heat 19837 in Figure 5, which show the ferrite is stable for all temperatures and increases in volume fraction as temperature decreases from the austenitization temperature. Thus, during cooling, the ferrite in the three alloys in Table 3 grows until the M_s temperature is reached. If the steels were directly quenched from austenitization, then the amount of ferrite calculated at the austenitization temperature would be expected to be much closer to the values. Because the carbon level of all three heats in Table 3 were below the specified limit, the amount of ferrite (greater than 50%) is most likely higher than would be expected for steels within the specification.

TABLE 3. Amount of Ferrite Present in Steels from Optical Microscopy

Heat Number	Alloy	Area Fraction (%) of Ferrite
19837	91	56
19839	92	59
19841	122	80

The effect of the ferrite on mechanical properties was dramatic. The tensile strength of these three alloys was significantly reduced compared to alloys without ferrite. Heat 19841, which had the highest volume fraction of ferrite had the lowest measured tensile strength both at room temperature and at 650°C. The creep-rupture results showed the P91 and P122 with ferrite had similar rupture strength below the minimum lifetimes predicted for P91. For P92, the life was reduced compared to the P92 without ferrite, but the rupture strength was higher than the other alloys with ferrite. It is unclear why the P92 with ferrite showed the highest tensile and rupture strength of the ferrite-

containing alloys. Perhaps the high level of W beyond the specified range contributed to increased strength of the ferrite, but additional work is necessary to explain these results.

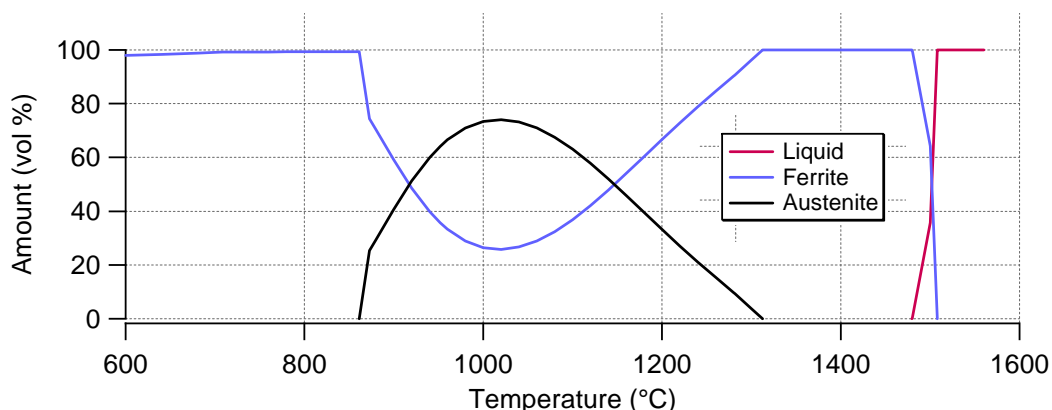


Figure 5. Calculated phase stability for liquid (red), ferrite (blue), and austenite (black) as a function of temperature for P91 Heat 19837.

To evaluate the critical temperature calculations, it is important to note the effect of heating rate when describing the transformation behavior of these steels. For the alloys with data at two heating rates, the A_{c1} temperature was 21°C lower for the slower heating rate of 2°C/min compared to the 100°C/min values. The thermodynamically calculated lower critical (equilibrium) temperature, A_1 which is the A_{c1} value at an infinitely slow heating rate (and the value determined in Thermocalc), was even lower than the 2°C/min values. This may explain why phase transformations have been observed below the A_{c1} temperatures in these alloys [9] where it is possible to heat-treat the alloy below an experimentally determined A_{c1} value (heating rate dependent) but heat-treat above the A_1 value. Thus, the A_1 value is a much more useful measurement for maximum heat-treatment temperature in comparison to A_{c1} .

A second important observation of the data in Table 2 is the comparison of the A_1 temperatures and the tempering temperature of 760°C. For P91 and P92, the A_1 temperature is above the tempering temperatures so no intercritical temperature excursion is expected. However, for P122 the A_1 temperature (but not the A_{c1} temperatures determined in this study) is below the tempering temperature. Thus during tempering of the P122, a fraction of the microstructure is expected to form austenite, which during subsequent cooling should produce ‘fresh’ untempered martensite.

The mechanical tests clearly indicate a difference in the low A_1 materials. The P91 and P92 with the 100% martensitic structure (Heats 19836 and 19838) show nearly identical tensile properties (strength and ductility) within the range expected for the alloys. However, the P122 (Heat 19840) showed much higher tensile strength than the other alloys presumably due to a microstructure containing untempered martensite. The tensile ductility of this heat was acceptable (in excess of 10%), which indicates only a portion of the microstructure is untempered martensite with brittle tensile behavior. The high-stress creep tests show longer than expected life. The creep strength of untempered martensite is expected to be higher than normalized-and-tempered material because the tempering process ‘softens’ the microstructure by reducing the dislocation density. However, the P122 mixed microstructure should also contain highly tempered martensite, which can be relatively weak. Thus longer-time testing at lower stresses may reduce the observed strengthening effect. Additionally, other important properties critical to fabrication of components, such as cold tensile ductility, fracture toughness, weldability, and Charpy impact, may be negatively affected by untempered martensite. Thus, longer-term creep test and additional property evaluation would be beneficial to understanding the behavior of such a mixed microstructure.

This study has shown the potential for computational thermodynamics to explain microstructural features in CSEF due to chemistry variations and heat-treatment temperatures. Specifically, the A_1 calculations have been shown to be more useful than the A_{c1} measurements in evaluation of the alloy transformation behavior. The current specification for P91 (ASTM A 387 Grade 91) states that “Grade 91 plates shall be normalized at 1040 to 1080°C and shall be tempered at 730 to 800°C.” The maximum tempering temperature of 800°C may be above the A_1 temperature for some heats of P91. To evaluate the A_1 temperature range, 1857 different chemical compositions were analyzed by CT. The chemistries were generated by choosing 5 compositions and varying one element at a time for the entire specification range. An additional ~ 50 heats taken from certified material test reports (CMTRs), laboratory produced heats, and the melting range of a major P91 material supplier were also analyzed. The results are shown as a histogram in Figure 6. The number of heats (counts) are not critical to the analysis, but rather, the predicted A_1 temperature range is of most interest. For the P91 specification range, the A_1 temperature is 766 to 856°C, which overlaps the specified tempering range for the alloy. Thus, within the current specification for P91, chemical compositions may be produced that when tempered according to the specification will exceed the lower critical temperature.

CT can provide a tool for setting chemical composition and heat-treatment limits. Figure 6 shows one approach to using CT. Utilizing the current specification range for P91, the 1857 chemistries were analyzed for Ni, Mn, Cr, and Si. Combining the alloying element effects, the compositions were limited to those with $Ni+Mn < 0.9$ wt % and $Cr+Si > 8.8$ wt %. The result of this restriction on the chemistry range was a tighter A_1 temperature range of 790 to 856°C. Thus, the current P91 specification could be altered to include this chemical composition restriction and a reduction in the maximum tempering temperature to 790°C which would eliminate the potential for tempering above the intercritical temperature regime. Alternate approaches, such as changing the existing ranges/maximums for some alloying elements, will have similar effects depending on the goal. A database is being generated for the potential for ferrite formation with the goal of performing a similar analysis. These results show that CT is a powerful tool for providing rational limits for chemistry and heat-treatment in these alloys.

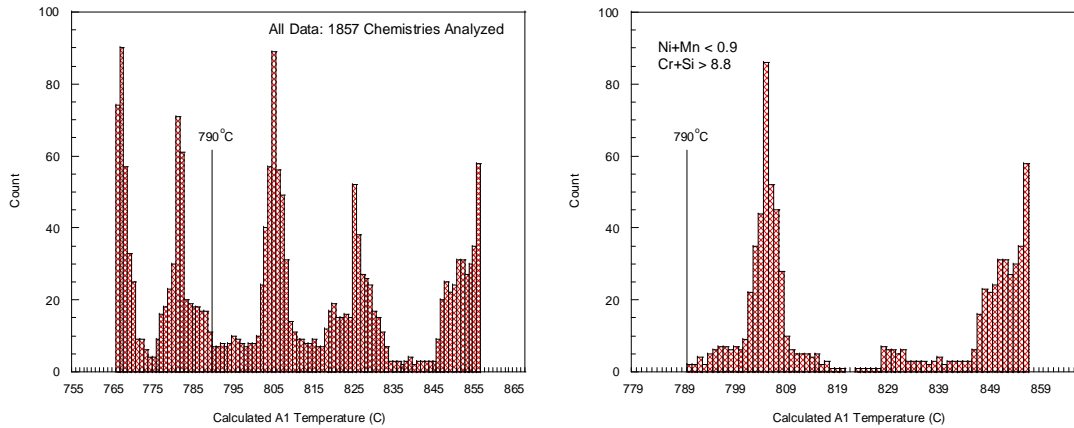


Figure 6. Calculated A_1 temperatures for over 1800 ASTM A387 Grade 91 compositions within the current specification range for the product chemistry (left) and for compositions within the current specification range when $Cr+Si > 8.8$ and $Ni+Mn < 0.9$ (right)

CONCLUSION

Experimental heats of P91, P92, and P122 were successfully produced at or slightly beyond the specification limits for the alloys. Optical microscopy and thermo-mechanical simulation confirmed the expected microstructural variations in the alloys, where after normalization and tempering one of each alloy contained ferrite and the other had a lower-- critical temperature (A_1) below 800°C. Tensile tests at room temperature and 650°C showed typical behavior for the P91 and P92 with the 100% tempered martensitic structure, but the P122 with 100% martensite showed much higher tensile strength due to untempered martensite that formed during tempering in the intercritical temperature regime. All materials with ferrite showed poor tensile strength. Subsize specimens were creep tested at 650°C for times up to 4,000 hours with some tests still in progress. The rupture results showed all the materials with ferrite had inferior creep strength compared with the low A_1 materials.

Using computational thermodynamics, a preliminary study of over 1800 potential compositions for P91 were analyzed. The results showed the minimum possible A_1 temperature for the specification range could be raised from 766°C to 790°C by minor restrictions on Cr+Si and Ni+Mn content. This study proves the usefulness of thermodynamic calculations for setting rational chemical composition ranges for CSEF steels to control the critical temperatures, set heat-treatment temperature limits, and eliminate the formation of ferrite.

ACKNOWLEDGEMENT

This research was supported by the U.S. Department of Energy (DOE), Office of Fossil Energy, Advanced Research Materials Program, under Contract DE-AC05-00OR22725 with UT-Battelle, LLC. Special thanks to Keely Wilson of Michigan Tech, and Ralph Martin and Alan Frederick of ORNL for their assistance with the experimental studies and to Ron Klueh for reviewing the manuscript.

REFERENCES

1. J.P. Shingledecker, M.L. Santella, R.L. Klueh. "Evaluation of heat-treatment temperatures and corresponding properties of improperly heat-treated Grade 91." *Proceedings of Industry and Research Experience in the Use of P/T91 and Other New Steels (London, UK - June 20-21, 2007). European Technology Development (ETD)*. CD-ROM
2. J. Parker. "Practical Experience with Advanced Steels." *Proceedings to the Fourth International Conference on Advances in Materials Technology for Fossil Power Plants (Hilton Head, SC, Oct. 25-28, 2004)*. ASM-International, Materials Park, OH, 2005. 231-246.
3. C. Petry. "Modeling creep rupture of P91 welds: application to life assessment of industrial components." *Proceedings of Industry and Research Experience in the Use of P/T91 and Other New Steels (London, UK - June 20-21, 2007). European Technology Development (ETD)*. CD-ROM
4. R. L. Klueh, J. P. Shingledecker. "Investigation of a Modified 9Cr-1Mo (P91) Pipe Failure. ORNL/TM-2006/1 Oak Ridge, TN (April 2006)
5. A. Shibli, D. Robertson. "Experience with the Use of P91 Steels in Power Plant Boilers." *Proceedings of the 5th International Conference on Advances in Materials Technology for Fossil Power Plants. (Marco Island, FL, Oct. 3-5, 2007)*
6. S.J. Brett, J.S. Bates, R.C. Thomson. "Aluminium Nitride Precipitation in Low Strength Grade 91 Power Plant Steels." *Proceedings to the Fourth International Conference on Advances in Materials Technology*

- for *Fossil Power Plants (Hilton Head, SC, Oct. 25-28, 2004)*. ASM-International, Materials Park, OH, 2005. 1183-1197.
7. K. Yoshida, T. Sato. *Presentation to ASME B&PV Code SG-Strength of Weldments*. New Orleans, LA (August 12, 2007).
 8. K. Kimura, K. Sawada, H. Kushima, Y. Toda. "Influence of Delta Ferrite Phase on Long-Term Creep Strength of High Chromium Ferritic Creep Resistant Steels." *7th International Charles Parsons Turbine Conference (Glasgow, UK, Sept. 11-13, 2007)*. Institute of Materials, London, UK, 2007.
 9. F. Masuyama, N. Nishimura. "Phase Transformation and Properties of Gr. 91 at Around Critical Temperature." *PVP-Vol. 476, Experience With Creep-Strength Enhanced Ferritic Steels and New and Emerging Computational Methods (San Diego, CA - June 25-29, 2004)*. PVP2004-2574. Am. Soc. Mech. Engin., New York, NY, 2007
 10. S.H. Ryu, Y.S. Lee, B.O. Kong, J.T. Kim. "A Study on the Variation of the Hardness and the Creep Rupture Strength with Thermal Histories in a Mod. 9Cr-1Mo Steel." *First Int. Conf. on Advanced Structural Steels (ICASS2002), May 22-24, 2002, Organized by NIMS, Tsukuba, Japan*.
 11. N. Saunders, "*Fe-DATA, a database for thermodynamic calculations for Fe alloys*," Thermotech Ltd., Surrey Technology Centre, The Surrey Research Park, Guilford, Surrey GU2 7YG, U.K